NASA TECHNICAL NOTE

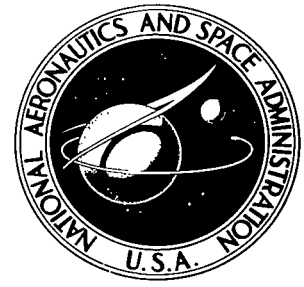

NASA TN D-8355

DIRECTIONALLY SOLIDIFIED EUTECTIC ALLOY γ-β

Surendra N. Tewari

Lewis Research Center
Cleveland, Ohio 44135

NATIONAL AERONAUTICS AND SPACE ADMINISTRATION • WASHINGTON, D. C. • JANUARY 1977

1. Report No.	2. Government Accession No.	3. Recipient's Catalog No.
NASA TN D-8355		

4. Title and Subtitle
DIRECTIONALLY SOLIDIFIED EUTECTIC ALLOY γ-β

5. Report Date
January 1977

6. Performing Organization Code

7. Author(s)
Surendra N. Tewari

8. Performing Organization Report No.
E-8845

9. Performing Organization Name and Address
Lewis Research Center
National Aeronautics and Space Administration
Cleveland, Ohio 44135

10. Work Unit No.
505-01

11. Contract or Grant No.

12. Sponsoring Agency Name and Address
National Aeronautics and Space Administration
Washington, D.C. 20546

13. Type of Report and Period Covered
Technical Note

14. Sponsoring Agency Code

15. Supplementary Notes
Presented in part at the 105th Annual Meeting of the American Institute of Mining, Metallurgical, and Petroleum Engineers, Las Vegas, Nevada, February 22-26, 1976.

16. Abstract

A pseudobinary eutectic alloy composition was determined by a previously developed bleed-out technique. The directionally solidified eutectic alloy with a composition of Ni-37.4Fe-10.0Cr-9.6Al (in wt%) had tensile strengths decreasing from 1090 MPa at room temperature to 54 MPa at 1100° C. The low density, excellent microstructural stability, and oxidation resistance of the alloy during thermal cycling suggest that it might have applicability as a gas-turbine vane alloy while its relatively low high-temperature strength precludes its use as a blade alloy. A zirconium addition increased the 750° C strength, and a tungsten addition was ineffective. The γ-β eutectic alloys appeared to obey a "normal freezing" relation.

17. Key Words (Suggested by Author(s))	18. Distribution Statement
Nickel alloys; Heat resistant alloys; Turbine blades; Mechanical properties; Eutectic alloys; Solidification; Microstructure; Ductility; Oxidation resistance	Unclassified - unlimited STAR Category 26

19. Security Classif. (of this report)	20. Security Classif. (of this page)	21. No. of Pages	22. Price*
Unclassified	Unclassified	27	$4.00

* For sale by the National Technical Information Service, Springfield, Virginia 22161

DIRECTIONALLY SOLIDIFIED EUTECTIC ALLOY γ-β

by Surendra N. Tewari*

Lewis Research Center

SUMMARY

The primary purpose of this research was to produce and evaluate a directionally solidified (DS) γ-β pseudobinary eutectic alloy, having first established and determined the composition of such an alloy by a previously developed bleed-out technique. The evaluation was intended to provide an indication of the suitability of the material for advanced gas turbine blade or vane materials.

The finally evolved alloy had a composition of Ni-37.4Fe-10.0Cr-9.6Al (in wt%) and, when directionally solidified, its structure consisted of alternating lamellae of γ, Fe-Ni solid solution, and β, (Fe,Ni)Al intermetallic phase. The crystallographic relations among γ, β and the alloy growth direction were

$$[110]_\gamma \parallel [111]_\beta \parallel \text{growth direction}$$

$$(111)_\gamma \parallel (110)_\beta$$

The alloy had tensile strengths of 1090 megapascals at room temperature, 360 megapascals at 750° C, and 54 megapascals at 1100° C. The alloy exhibited high elongations, 17 percent at room temperature, 36 percent at 750° C, and 95 percent at 1100° C. Its density was very low, 7.5 grams per cubic centimeter. The alloy showed excellent microstructural stability during thermal cycling (1800 cycles from 1100° to 425° C) and very good oxidation resistance.

An attempt was made to increase the strength of the alloy at 750° C by adding 1 weight percent tungsten or 0.6 weight percent zirconium. The tungsten addition did not result in a strength increase. The zirconium modified alloy showed about a 50 percent increase in strength at 750° C. However, the zirconium modified alloy did not form an alined structure at growth speeds greater than 1 centimeter per hour, compared with 2 centimeters per hour for the base composition alloy and the tungsten modified alloy.

The results of the investigation suggest that the γ-β DS eutectic alloy would not be suitable for gas-turbine-blade applications. However, it may have potential as a vane alloy.

*National Research Council - National Aeronautics and Space Administration Research Associate.

INTRODUCTION

Directionally solidified (DS) superalloy eutectics are being considered as the next generation material for aircraft gas-turbine blades. Their use is expected to result in significant improvement in engine performance due to a projected 50° to 100° C increase in allowable metal temperatures over those of conventionally cast superalloys (ref. 1). This would result in reduced fuel consumption and increased power output. The DS eutectic alloys under investigation range from ductile-ductile systems, where both the matrix and the reinforcing phases are ductile, to brittle-brittle systems, where both phases are brittle (ref. 2). Even though engine designers have shown a tendency to accept lower ductility materials for turbine-blade application, the brittle-brittle systems are not likely to be acceptable in the immediate future. The DS eutectic alloys most seriously being considered for turbine-blade application are from ductile-brittle systems (ref. 2). Lamellar, intermetallic-(Ni_3Nb) reinforced nickel-base alloys (ref. 3) and fibrous, monocarbide (TaC), reinforced nickel and cobalt base alloys (ref. 4) have probably received the most intensive investigation. Both systems lack adequate oxidation resistance and would require protective coatings.

Low density, high tensile and stress rupture strengths at high temperature, microstructural stability during thermal cycling, and adequate oxidation resistance are the initial properties sought by turbine-blade designers. A literature search of various systems capable of forming high-melting-point eutectics revealed that a pseudobinary eutectic between γ, an iron-nickel (Fe-Ni) solid solution, and β, an iron-nickel-aluminum (Fe-Ni-Al) intermetallic, system had been found (ref. 5). This ductile-brittle system seemed an attractive possibility for meeting the property criteria. The oxidation resistance of the alloy should be further increased by the addition of chromium. The purpose of this investigation was to determine a γ-β eutectic alloy composition in a Fe-Ni-Cr-Al system, to directionally solidify it, and to determine its suitability for advanced gas-turbine blade or vane applications.

The eutectic composition in the Fe-Ni-Al system reported in the literature was modified by a chromium addition. A casting of the modified composition alloy was melted using a modified Bridgman furnace, and, using a eutectic bleed-out technique (ref. 6), the composition of a first approximation eutectic alloy was determined. This composition, in turn, was directionally solidified and chemically and microstructurally analyzed. The chemistry of the alined zone of the DS bar was selected for the first melt, which in turn was directionally solidified and tested. Its crystallography and microstructural stability during thermal cycling were evaluated. The temperature dependence of the tensile properties was determined, and a limited attempt was made to increase the tensile strength by additions of tungsten and zirconium to the alloy.

MATERIALS, APPARATUS, AND PROCEDURE

Materials

The purities of raw materials used in this study are shown in table I.

Apparatus

The directional solidification apparatus, which is a modified Bridgman furnace, is shown in figure 1. The crucible containing the ingot was heated by radiation from a graphite susceptor positioned inside an induction coil. The alumina heat shield surrounding the graphite susceptor was used to minimize the heat loss from the susceptor. The power was supplied by a 7.5 kilowatt radiofrequency generator operating at 400 kilohertz. For any given power setting a flat solid-liquid interface was obtained just below the induction coil by adjusting the thickness of the alumina spacer between the susceptor and water chill ring. The induction coil was more densely wound at the bottom to provide greater localized heating at the solid-liquid interface.

Procedure

Master melting. - Initial 1.2-kilogram heats were melted in a 50-kilowatt, 10-kilohertz induction furnace in calcia-stabilized zirconia crucibles. The environment was first evacuated then partially backfilled with argon. The melts were poured into preheated zircon shell molds to make cylindrical bar ingots (1 cm in diam, 16-cm long) for subsequent directional solidification. Each shell mold provided six bar ingots.

Bleed-out and eutectic composition determination. - The approximate eutectic composition was obtained by the eutectic bleed-out technique (ref. 6). A bar ingot of the off-eutectic composition alloy was slowly heated in the Bridgman furnace. The eutectic regions on the bar surface, being the lowest melting point constituents, melted first and solidified in a sleeve-like shape at the bottom of the bar. This eutectic bleed-out material was analyzed by spectrochemical analysis and thus the first approximation of the eutectic alloy composition was obtained.

This first approximation eutectic alloy composition was master-melted and cast. The bar ingot thus obtained was then directionally solidified at 1 centimeter per hour. (See the next section.) Several 0.3-centimeter-thick disks were cut at 1-centimeter intervals along the DS bar length, analyzed by wet chemical analysis, and examined metallographically. Wet chemical analysis of the well alined region of the DS bar yielded the final base-alloy composition selected for the subsequent directional solidification and property evaluation.

Directional solidification. - The bar ingots obtained from the master melt of the final base-alloy composition were remelted and directionally solidified in an alumina tube crucible (1.3 cm i.d., 1.8 cm o.d., 30 cm long) in the modified Bridgman furnace (fig. 1) under a flowing argon atmosphere. Directional solidification was obtained by lowering the crucible through a water-spray chill ring at a constant speed of 1 or 2 centimeters per hour. The temperature gradient in the liquid at the liquid-solid interface was determined to be about 200° to 250° C per centimeter. The melts were maintained at a superheat of about 350° C. No mold-metal reaction was observed after the directional solidification which took up to 15 hours. Typical DS bars were 10 centimeters long. Twelve bars were directionally solidified. Each DS bar yielded one specimen for mechanical testing.

Mechanical testing. - A flat was ground on the DS bar surface along its length, polished, and etched by immersing it 3 seconds in a solution of 100 milliliters water, 100 milliliters hydrochloric acid, 30 grams of ferric chloride, and 10 grams of cupric chloride to observe the degree of alinement along the DS bar length. Directionally solidified bars showing well alined microstructure were ground to the specimen dimensions shown in figure 2. Machined specimens were inspected by X-ray radiography and fluorescent dye penetrant to detect any internal or surface voids or cracks. Tensile tests were conducted from 25° to 1100° C in air at a constant crosshead speed of 1.2 centimeters per minute. All tests were loaded parallel to the alloy growth direction.

Thermal cycling. - The 1.2-centimeter-diameter DS bar was subjected to thermal cycling in a burner rig apparatus similar to the one used by Johnston and Ashbrook (ref. 7). The bar (or specimen) was heated to 1100° C in the Mach 0.3 blast of a combusted gas stream achieved by burning a mixture of JP-5 grade jet fuel and air. The bar (or specimen) was held in the jet for 2 minutes and then cooled to 425° C in a Mach 0.7 blast of room-temperature air. The total elapsed time for one cycle was 3 minutes. The bar was taken out at regular intervals and weighed to record the weight loss as a function of number of cycles.

Metallography. - The microstructure and alinement of the DS alloys were examined by light metallography. Specimens mounted in Bakelite were polished using normal metallographic procedures with a final polish of 0.5-micrometer alumina on microcloth. Specimens were etched in the same etchant which was used for inspection. Scanning electron microscopy (SEM) was used for fracture examination. Crystallographic relations among γ, β and the alloy growth direction were investigated by transmission electron microscopy (see the appendix).

RESULTS AND DISCUSSION

Eutectic Composition and Growth Morphology

The γ-β eutectic composition reported in the Fe-Ni-Al system (ref. 5) was modified by adding 10 weight percent chromium. The eutectic bleed-out technique (ref. 6) on this composition yielded the first approximation eutectic alloy, Ni-36Fe-9.3Cr-8.7Al[1] (wet chemical analysis). The bar ingots of this composition when directionally solidified at 1 centimeter per hour had the microstructure shown in figure 3. These are transverse sections (perpendicular to the growth direction) along the length of the DS bar. The microstructure near the bottom of the first approximation DS bar contained more than 50 volume percent proeutectic γ phase. Although the alloy composition here was obviously off-eutectic, the γ-β lamellae in the eutectic region were observed to be alined along the growth direction. As the solidification progressed, the amount of eutectic region continuously increased and finally reached a 100 percent alined structure at 5.5 centimeters from the bottom. There was no change in microstructure from this point to about 2 centimeters from the top of the bar where a cellular microstructure (less than 100 % lamellar) developed due to the changed temperature gradient at the solid-liquid interface.

Figure 4 shows the change in alloy composition of the first approximation alloy along the DS bar length, which had resulted in the microstructural observation described previously. As solidification progressed the aluminum, chromium, iron, and nickel contents in the melt changed continuously, seeking a eutectic composition. At about 7 centimeters from the bottom, the compositions appear to be leveling out. This observation along with the microstructural observations (fig. 3) would indicate that a near eutectic composition was reached by the time that about 7 centimeters of the bar length had directionally solidified.

Based on the wet chemical analysis of the well alined region of the DS bar (fig. 4), the charge composition of Ni-34.0Fe-9.8Cr-9.2Al was selected for the final base alloy. The resulting DS bar had an average composition of Ni-37.4Fe-10.0Cr-9.6Al. The liquidus and solidus temperatures for this alloy, measured by differential thermal analysis, gave a freezing range from 1383° to 1341° C (fig. 5). This indicates that the alloy is still not an exact eutectic. However, when this base alloy was directionally solidified at 2 centimeters per hour, a well alined lamellar microstructure occurred along the entire DS bar length. Figure 6 shows typical transverse and longitudinal sections from such a DS bar. The DS eutectic alloy contains alternating lamellae of γ and β phases. The average volume fraction of the β phase in the base composition alloy observed by quantitative scanning television microscopy (ref. 8) of scanning electron

[1]This composition resulted from melting the charge composition of Ni-36.0Fe-9.4Cr-8.9Al.

micrographs (transverse sections) was 0.40. According to the predictions based on the volume fraction of the second phase, the microstructure is expected to be lamellar when the volume fraction of the second phase exceeds 0.28 (ref. 9).

The chemical-analysis along the length of a DS bar of the final base alloy composition is shown in figure 7. It may be noted that the elemental compositions are nearly constant along the DS bar length.

Composition and crystal structure of γ and β phases. - The average compositions of the γ and β phases as determined by electron probe microanalysis were Ni-45.1Fe-10.8Cr-6.1Al and Ni-24.5Fe-3.5Cr-13.9Al, respectively. X-ray diffraction analysis (copper K-α radiation, 40 kV, 45 mA) of the DS eutectic alloy showed the presence of face centered cubic (fcc) γ matrix with a lattice parameter of 3.597 angstroms and a CsCl type of body centered cubic β phase with a lattice parameter of 2.884 angstroms.

Crystallographic orientation relations. - The crystallographic relations among γ, β and the alloy growth direction were determined (see the appendix):

$$[110]_\gamma \parallel [111]_\beta \parallel \text{growth direction}$$

$$(111)_\gamma \parallel (110)_\beta$$

Tensile Properties of γ-β Eutectic Alloys

Base alloy composition. - The temperature dependence of the tensile properties is shown in figure 8. The ultimate tensile strength of the alloy decreased with increasing temperature from 1090 megapascals at room temperature to about 54 megapascals at 1100° C. The yield strength (0.2 % offset) at room temperature was about 60 percent of the ultimate strength for the alloy (table II). However, as the temperature was raised to 1100° C, the yield strength became almost equal to the ultimate strength. The tensile elongations shown in figure 8 are the plastic elongations as observed on the load against elongation plots. At room temperature the elongation is about 17 percent. It increases with the increasing temperature, and at 1100° C it is about 95 percent. Reduction in area values are also high as shown in table II.

For comparison the tensile strengths of $\gamma/\gamma' - \delta$ (ref. 3) are also shown in figure 8. It is obvious that the high-temperature strengths of the γ-β alloy of this study are far less than those of the $\gamma/\gamma' - \delta$ alloy. The γ-β eutectic alloy is therefore not considered suitable for gas-turbine blade applications. The low strength of the γ-β alloys at high temperature may be due to the fact that the β phase becomes very weak and ductile at high temperatures. This possibility is suggested by reference 10, which gives strengths of the nickel-aluminum (NiAl) intermetallic compound (an isomorph of the β

phase of this study as noted earlier). In this study (ref. 10) it was shown that at about 1100° C polycrystalline NiAl had trength of about 28 megapascals. At this temperature the material became exceed .y plastic, deforming drastically with no increase in load. In essence, the NiAl faile 28 megapascals.

One final property comparis... should be made. Before this investigation was started, the results of another investigation on a γ-β eutectic with an appreciably different composition (Ni-10.8Fe-20.1Cr-8.9Al) from that of this study were published (ref. 11). This alloy had almost identical tensile properties at room temperature and 1100° C but more strength at 750° C.

Microstructural features of tensile-fracture in the γ-β DS eutectic alloy of the base composition at room temperature and 1100° C are shown in figure 9. A longitudinal section through the room-temperature tensile fracture (fig. 9(a)) shows fracture of brittle β lamellae between the ductile necked regions of γ. The cleavage surfaces in β are perpendicular to the lamellae orientation. The β lamellae were also observed to split and crack occasionally in the region immediately below the fracture surface. Figure 9(b), a scanning electron micrograph of the fracture surface, shows more clearly the ductile failure of the γ lamellae, which resulted in extensive necking, and the brittle failure of the β lamellae with flat fracture ends. No twinning or slip was observed in β lamellae by light metallography. A brittle failure of β phase raises an interesting question. Since very little cracking was observed in the gage section, how was the observed 17-percent alloy ductility at room temperature accommodated in the β lamellae?

In model system studies of artificially made composites in tungeten-reinforced-copper fiber and laminated composites, fracture of the relatively brittle tungsten phase occurred first, but the adjacent copper gripped the tungsten segments and allowed this composite to increase in strength at a reduced rate as elongation of the specimen continued (ref. 12). The net result was that the composite as a whole appeared to have failed in a ductile mode. The same phenomenon could be expected to occur during room-temperature tensile fracture of the γ-β eutectic of this study and thus would seem to be a logical explanation of the high room-temperature ductility. However, the fact that cracks in the β phase were found only in the immediate vicinity of the matrix fracture surface suggests that the cracking was not progressive as was the fracture of tungsten in the model system just described. How then was the observed 17 percent elongation in room-temperature tensile tests accommodated in the γ-β DS eutectic? This question can not be answered from the results of this investigation. If the strengths and moduli of elasticities of the actual single crystals constituting the eutectic could be calculated, or if strengths and ductilities of single-crystal isomorphs of these phases were known, it would be possible to speculate on the cause of the appreciable ductility of the DS alloys of this investigation. Transmission electron microscopy of the specimens taken from the gage section of the tensile specimens or metallographic examination of interrupted

tensile tests would also shed more light on the mechanism involved in the failure of the β lamellae.

Elevated temperature fracture (fig. 9(c)) on the other hand, shows extensive bending and ductility of both the γ and β lamellae. Stress-assisted coarsening and spheroidization of β lamellae were observed near the fracture end. Such spheroidization has also been observed during elevated temperature long-time stress rupture tests of $\gamma/\gamma' - \delta$ DS eutectic alloys (ref. 3).

Modified γ-β composition alloys. - In this investigation an attempt was made to increase the γ-β alloy strength by adding 1 weight percent tungsten or 0.6 weight percent zirconium to the base composition. Tungsten is known to be a potent solid solution strengthener for iron and nickel base superalloys (ref. 13), and its addition may be expected to strengthen the γ phase. Zirconium is an effective strengthener of NiAl (ref. 14). Minor element additions, however, were expected to change the alloy freezing range and to require different solidification conditions to obtain an alined microstructure. Hence, the additions were kept to relatively low amounts.

The 1 percent tungsten modified alloy, when directionally solidified at 2 centimeters per hour in a temperature gradient of about 200° C per centimeter at the solid-liquid interface, yielded an alined microstructure. However, measurements at 750° C did not show an improvement in alloy tensile strength over the base alloy (table II, fig. 8).

The tensile strength at 750° C of the DS alloy modified with 0.6 percent zirconium was 478 megapascals. This was about 35 percent above that given previously for the base alloy eutectic. However, it was necessary to solidify the zirconium modified alloy at the rate of 1 centimeter per hour to achieve an alined structure. Since it is known that tensile strengths of DS eutectic alloys increase with increasing solidification rate (ref. 15), meaningful strength comparisons can be made only between the alloys solidified under the same growth conditions. The 0.6 percent zirconium modified alloy showed at 750° C about a 50-percent strength increase over the base alloy solidified at 1 centimeter per hour (table II, fig. 8). However, even the 750° C strength of the modified γ-β alloy was considerably less than that of the DS $\gamma/\gamma' - \delta$ eutectic alloys. The γ-β alloys are therefore not considered suitable for gas-turbine-blade applications.

Effect of Thermal Cycling

Resistance of the microstructure to thermal cycling damage is an important parameter for turbine blade and vane alloys. The DS γ-β eutectic alloy was therefore subjected to thermal cycling in air between 425° and 1100° C, using 3-minute cycles. After 1800 cycles the microstructure of the alloy was examined. No microstructural change was observed, except for some rounding off of sharp corners of β lamellae (fig. 10).

A β denuded zone about 20 micrometers deep was observed at the alloy surface (fig. 10(c)). This zone apparently developed because of aluminum diffusion to the surface. The aluminum depletion from the β phase changed the β region to γ.

No systematic study was made of the oxidation resistance of the alloy. However, the weight loss that occurred during the thermal cycling was measured. The results are shown in figure 11. The γ-β eutectic alloy examined has much better oxidation resistance than γ/γ' - δ DS eutectic alloy (ref. 16), and it compares favorably with B-1900 which was subjected to similar thermal cycling treatment (ref. 16).

The directionally solidified off-eutectic (the first approximation alloy) composition alloy (3 cm from the bottom, figs. 3 and 4) was also subjected to the same thermal cycling treatment. The change in microstructure following 1800 thermal cycles is shown in figure 12. These are transverse sections at about 3 centimeters from the bottom of the DS bar. Thermal cycling resulted in precipitation of what are presumably β platelets in cellular γ regions. During directional solidification cellular γ regions grow more rapidly than the lamellar γ-β regions. This results in a composition difference between cellular and lamellar γ regions. Electron microprobe analysis of adjacent cellular and lamellar γ regions in DS alloy (fig. 12(a)) showed the compositions to be Ni-39Fe-11Cr-11Al and Fe-37Ni-13Cr-8Al (in at. %), respectively. Apparently this small difference in composition makes the cellular γ regions unstable during thermal cycling.

Elemental Segregation Due to Directional Solidification

Pfann (ref. 17) has shown that the elemental segregation due to "normal freezing" (progressive plane front solidification of entire melt) or single-phase alloys follows the mathematical relation,

$$C = C_o k'(1 - g)^{(k-1)} \tag{1}$$

where C is the composition in the solid corresponding to fraction solidified up to the point g; C_o is the initial bulk average composition, and k is a distribution coefficient (the ratio of the elemental composition of solid and the liquid under equilibrium solidification). Recently Gigliotti and Henry (ref. 18) showed that the elemental segregation along the length of a DS fibrous eutectic alloy, γ/γ' - TaC, also follows the same mathematical relation. Their γ/γ' - TaC alloy was off-eutectic as evidenced by the presence of a sort-out zone of primary carbides in their DS bars. A sort-out zone is the volume of the melt solidifying initially where proeutectic phases solidify in a nonalined manner. The applicability of this relation was examined to determine whether the lamellar γ-β eutectic alloy system would obey the normal freezing relation. The data of figure 4 (the

off-eutectic first approximation γ-β alloy) for aluminum, chromium, and iron composition profiles were used for the analysis.

According to equation (1) a log (C/C_0) against log (1 - g) plot should be a straight line with a slope of k - 1 and an intercept of log k. A least squares straight line fit was made for each element on a log (C/C_0) against log (1 - g) plot (not shown here). The k values obtained from the slope and intercept of these plots were averaged to obtain the distribution coefficient k for each element (k values obtained from the slope and intercept differed from each other by less than 2 %). The results of such an analysis are shown in figure 13 in a Cartesian coordinate plot. A good fit can be observed between the experimental data points and the composition profile obtained from equation (1), that is, the solid lines. The distribution coefficient values vary from 0.9 to 1.08, which indicates that the alloy has a near eutectic composition.

The chemical analysis along the length of a DS bar of the finally determined base alloy composition is shown in figure 7. It may be noted that the elemental compositions are nearly constant along the DS bar length. The analysis of these compositions according to equation (1) gave k values of 0.99, 1.01, and 1.01 for aluminum, chromium, and iron, respectively.

These observations suggest that normal freezing analysis of Pfann (ref. 17) is also valid for plane front solidification of lamellar eutectic alloys.

CONCLUDING REMARKS

The γ-β DS eutectic alloys have relatively low elevated temperature tensile strength and are not considered suitable for application as an aircraft gas-turbine-blade material. On the other hand, the excellent resistance of the alloy to oxidation and thermal cycling damage, low density, plus the outstanding ductility of the alloy, suggest that it may have potential as gas-turbine-vane alloy where much lower stress levels are encountered. Further attempts to strengthen an alloy of the γ-β type may therefore be warranted.

SUMMARY OF RESULTS

This investigation, which was conducted to produce and evaluate a directionally solidified γ-β pseudobinary eutectic alloy, yielded the following results:

1. The composition of the base alloy γ-β eutectic, determined by a bleed-out technique and composition of a well-alined region in a first-approximation DS eutectic bar, was Ni-37.4Fe-10.0Cr-9.6Al (in wt%).

2. The alloy had a freezing range from 1383° to 1341° C and a density of 7.5 grams per cubic centimeter. The directionally solidified γ-β eutectic alloy had a microstruc-

ture consisting of alternating lamellae of γ (face centered cubic Fe-Ni solid solution) and β (CsCl type body centered cubic (Fe,Ni)Al) phases. Crystallographic relation among γ, β and the alloy growth direction were

$$[110]_\gamma \parallel [111]_\beta \parallel \text{growth direction}$$

$$(111)_\gamma \parallel (110)_\beta$$

3. The tensile strength of the alloy decreased from 1090 megapascals at room temperature to about 54 megapascals at 1100° C. Its tensile elongation increased from 17 percent at room temperature to about 95 percent at 1100° C.

4. The γ-β eutectic alloy did not show any microstructural degradation following 1800 thermal cycles (3-min cycles) from 1100° to 425° C. Its oxidation resistance was much better than that of the DS γ/γ' - δ eutectic alloys.

5. A 1-percent tungsten addition did not increase the alloy strength. A zirconium addition of 0.6 percent showed about a 50-percent strength increase at 750° C. However, the zirconium modified alloy did not yield an alined microstructure at growth speeds more than 1 centimeter per hour.

6. A mathematical analysis of the elemental segregation along the length of a directionally solidified bar indicated that the first-approximation alloy (Ni-36.0Fe-9.3Cr-8.7Al) followed a normal freezing relation. The base composition γ-β eutectic alloy also appeared to follow this relation.

Lewis Research Center,
National Aeronautics and Space Administration
Cleveland, Ohio, August 12, 1976,
505-01.

APPENDIX - CRYSTALLOGRAPHY OF γ-β DIRECTIONALLY SOLIDIFIED EUTECTIC

Small disks (3-mm diam) were electrical-discharge machined from thin transverse slices (0.02-cm thick) obtained from the directionally solidified Ni-37.4Fe-10.0Cr-9.6Al γ-β eutectic alloy. The disks were hand ground down to a thickness of about 50 micrometers on 600 grit paper. An electropolishing technique with two submerged jets, one from either side of the disk, was used to obtain the electron microscopy thin foils. The electropolishing was done at -70° C, 100 volts, and 5 milliamperes, in a solution consisting of 400 milliliters of ethyl alcohol, 70 milliliters of butylcellusolve, and 12 milliliters of perchloric acid.

An electron diffraction pattern taken on the γ-β interface is shown in figure 14. The γ spots are enclosed in squares, the β spots are enclosed in circles, and the Miller indices of the corresponding diffraction planes, hk$l$, are enclosed in parentheses. Analysis of the two sets of diffraction spots corresponding to β and γ phases is shown in table III. Assuming $[111]_\beta \parallel [110]_\gamma \parallel$ growth direction, the observed interplanar spacing ratios and angles between various spots show good agreement with the calculated values for β and γ (table III(a) and (b)) phases. Table III(c) compares experimentally observed and calculated β and γ interplanar spacing ratios and shows the good agreement between the two. It can be observed that $(111)_\gamma$ planes are parallel to $(011)_\beta$ planes (fig. 14).

REFERENCES

1. Jahnke, L. P.; and Bruch, C. A.: Requirements for and Characteristics Demanded of High Temperature Gas Turbine Components. Specialists Meeting on Directionally Solidified In Situ Composites. AGARD CP-156, 1974, pp. 3-12.

2. Ashbrook, R. L.: Directionally Solidified Composite Systems Under Evaluation. Specialists Meeting on Directionally Solidified In Situ Composites. AGARD CP-156, 1974, pp. 93-115.

3. Lemkey, F. D.: Eutectic Superalloys Strengthened by δ, Ni_3Cb Lamellae and γ', Ni_3Al Precipitates. NASA CR-2278, 1973.

4. Bibring, H.: Mechanical Behavior of Unidirectionally Solidified Composites. Proceedings of Conference on In-Situ Composites, vol. 2. National Research Council, 1972, pp. 1-69.

5. Metals Handbook vol. 8, 8th ed., Am. Soc. Metals, 1973.

6. Kim, Y. G.; and Ashbrook, R. L.: Directionally Solidified Pseudobinary Eutectics of Ni-Cr-(Hf-Zr). NASA TM X-71765, 1975.

7. Johnston, James R.; and Ashbrook, Richard L.: Oxidation and Thermal Fatigue Cracking of Nickel- and Cobalt-Base Alloys in a High Velocity Gas Stream. NASA TN D-5376, 1969.

8. Underwood, Ervin E.: Quantitative Stereology. Addison-Wesley, 1970, p. 173.

9. Cooksey, D. J. S.; et al.: The Freezing of Some Continuous Binary Eutectic Mixtures. Phil. Mag., vol. 10, no. 107, Nov. 1964, pp. 745-769.

10. Roznev, A. G.; and Wasilewski, R. J.: Tensile Properties of NiAl and NiTi. J. Inst. Metals, vol. 94, 1966, pp. 169-175.

11. Jackson, M. R.: The Ni-Cr-Al-Fe (γ-β) Eutectic System. Presented at the Conference on In Situ Composites - II. Bolton Landing, N.Y., Sept. 2-5, 1975.

12. Hoffman, Charles A.; and Weeton, John W.: Tensile Behavior of Unnotched and Notched Tungsten-Copper Laminar Composites. NASA TN D-8254, 1976.

13. Stoloff, N. S.: Fundamentals of Strengthening. The Superalloys. Chester Sims and William C. Hagel, eds., John Wiley & Sons, Inc., 1972, pp. 81-83.

14. Lawley, Alan: Mechanical Properties-Plastic Behavior. Intermetallic Compounds. J. H. Westbrook, ed., John Wiley & Sons, Inc., 1967, pp. 464-490.

15. Gell, M.; and Barkalow, R. H.: Microstructure-Property Relationship of a Directionally Solidified Superalloy Eutectic. The Microstructure and Design of Alloys, vol. 1, Metals Soc. (London), 1973, pp. 261-265.

16. Gray, H. R.; and Sanders, W. A.: Effect of Thermal Cycling in a Mach 0.3 Burner Rig on Properties and Structure of Directionally Solidified γ/γ' - δ Eutectic. Presented at Conference on In Situ Composites - II, Bolton Landing, N.Y., Sept. 2-5, 1975.

17. Pfann, W. G.: Redistribution of Solute During Freezing Liquid Metals and Solidification. Liquid Metals and Solidification. Am. Soc. Metals, 1958, pp. 218-242.

18. Gigliotti, M. F. X.; and Henry, M. F.: Segregation in a Plane Front Solidified γ/γ' - MC Alloy. Presented at Conference on In Situ Composites - II, Bolton Landing, N.Y., Sept. 2-5, 1975.

TABLE I. - RAW MATERIALS

Elements	Purity, wt%	Form
Ni	99.9	Electrolytic chips
Cr	99.8	Electrolytic chips
Fe	99.8	Chips
Al	99.9	Chips

TABLE II. - TENSILE PROPERTIES OF γ-β DIRECTIONALLY SOLIDIFIED EUTECTIC ALLOY

Charge composition, wt%	Growth rate, cm/hr	Temperature, °C	Tensile strength, MPa	0.2 % Yield strength, MPa	Elongation, percent	Reduction in area, percent
Ni-34.0Fe-9.8Cr-9.3Al	2	25	1051	652	19	19
	↓	25	1135	657	15	10
		750	363	337	37	59
		750	354	343	35	76
		1100	54	54	95	96
	1	750	283	266	33	48
Ni-34.0Fe-9.3Cr-9.0Al-1.0W	2	750	368	326	39	69
Ni-34.1Fe-9.3Cr-9.1Al-0.6Zr	1	750	478	398	32	77

TABLE III. - ORIENTATION RELATION BETWEEN γ AND β PHASES[a]

(a) β spots (enclosed in circles in fig. 14)

Spot number	Observed			Calculated		
	Radius, r, cm	r/r_4	Angle between spot 4 and other spots, deg	Miller indices, hkl	$\frac{d_{1\bar{1}0}}{d_{hkl}}$	Angle between (hkl) and $(1\bar{1}0)$, deg
1	1.08	0.99	180	$\bar{1}10$	1.0	180
2	1.09	1.0	120	$\bar{1}01$	↓	120
3	1.10	1.0	60	$0\bar{1}1$	↓	60
4	1.09	1.0	0	$1\bar{1}0$	↓	0
5	1.11	1.02	-59.5	$10\bar{1}$	↓	-60
6	1.07	.98	-120	$01\bar{1}$	↓	-120
7	1.88	1.73	90	$\bar{1}\bar{1}2$	1.73	90
8	1.88	1.73	30	$1\bar{2}1$	↓	30
9	1.90	1.74	-30	$2\bar{1}\bar{1}$	↓	-30
10	1.90	1.74	-151	$\bar{1}2\bar{1}$	↓	-150
11	1.88	1.73	150	$\bar{2}11$	↓	150
12	1.90	1.74	-90	$1\bar{1}\bar{2}$	↓	-90

(b) γ spots (enclosed in squares in fig. 14)

Spot number	Observed			Calculated		
	Radius, r, cm	$r/^b1.09$	Angle between spot 6 and other spots, deg	Miller indices, hkl	$\frac{d_{\bar{1}1\bar{1}}}{d_{hkl}}$	Angle between (hkl) and $(2\bar{2}0)$, deg
1	1.12	1.02	-145	$\bar{1}1\bar{1}$	1.0	-145
2	1.06	.97	-35	$1\bar{1}\bar{1}$	1.0	-35
3	1.10	1.01	35	$1\bar{1}1$	1.0	35
4	1.24	1.13	90	002	1.15	90
5	1.24	1.13	-90	$00\bar{2}$	1.15	-90
6	1.75	1.60	0	$2\bar{2}0$	1.63	0
7	2.12	1.94	-35	$2\bar{2}\bar{2}$	2.0	-35
8	2.15	1.97	35	$2\bar{2}2$	2.0	35
9	2.09	1.91	-115.5	$\bar{1}1\bar{3}$	1.91	-115

(c) Comparison of observed and calculated β and γ interplanar spacing ratios

Ratio of Miller indices, $(hkl)_\beta/(hkl)_\gamma$	Interplanar spacing ratio	
	Observed	Calculated (c)
110/111	1.0	0.98
112/111	.58	.57

[a]Plate 4167.

[b]1.09 is average of γ_1, γ_2, and γ_3.

[c]$a_{o\gamma}$ = 0.597 Å, $a_{o\beta}$ = 2.884 Å.

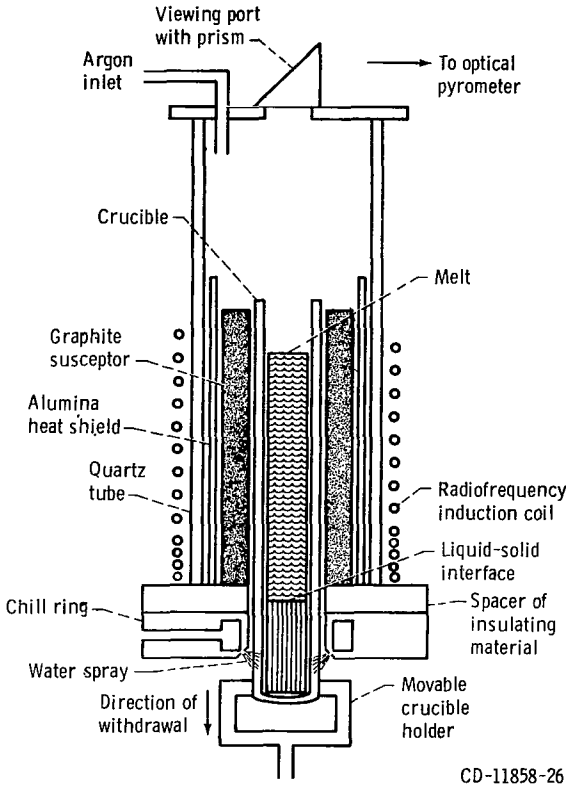

Figure 1. - Bridgman directional solidification apparatus.

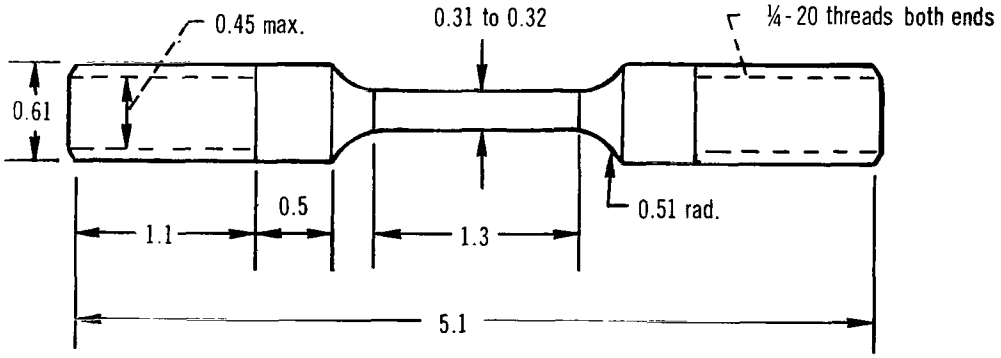

Figure 2. - Tensile test specimen. (Dimensions are in cm.)

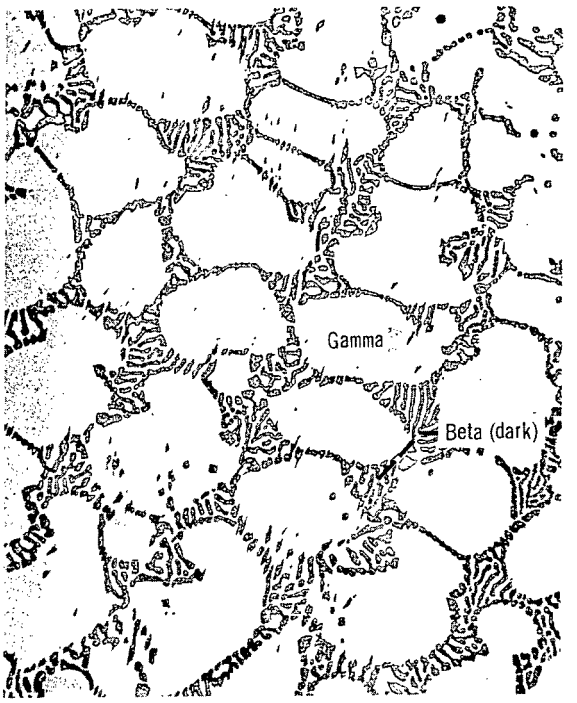

(a) Distance from bottom of bar, 1.5 centimeters.

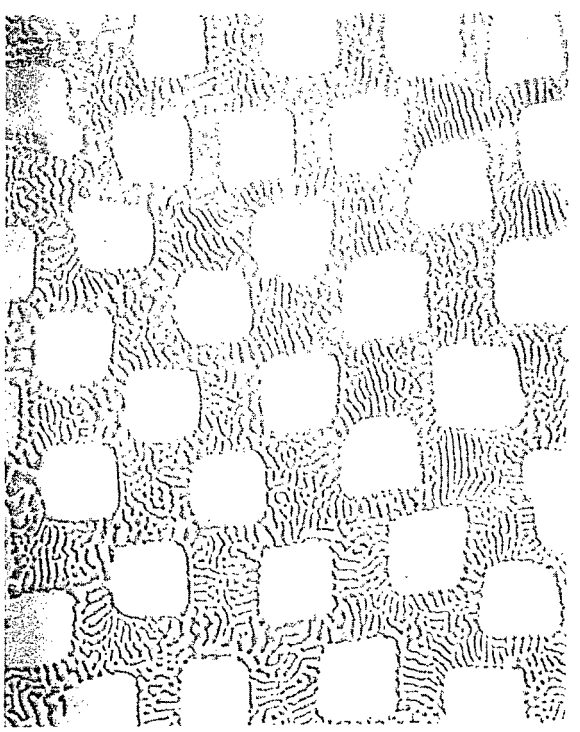

(b) Distance from bottom of bar, 3.5 centimeters.

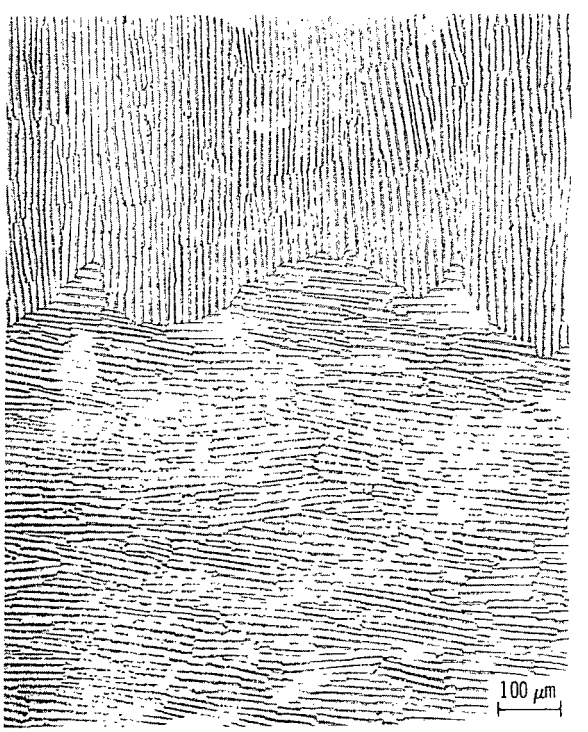

(c) Distance from bottom of bar, 5.5 centimeters.

Figure 3. - Change in microstructure of a directionally solidified alloy with the nominal composition 46.0 Ni-36.0Fe-9.3Cr-8.7Al (in wt %) as function of distance from bottom of bar (transverse sections).

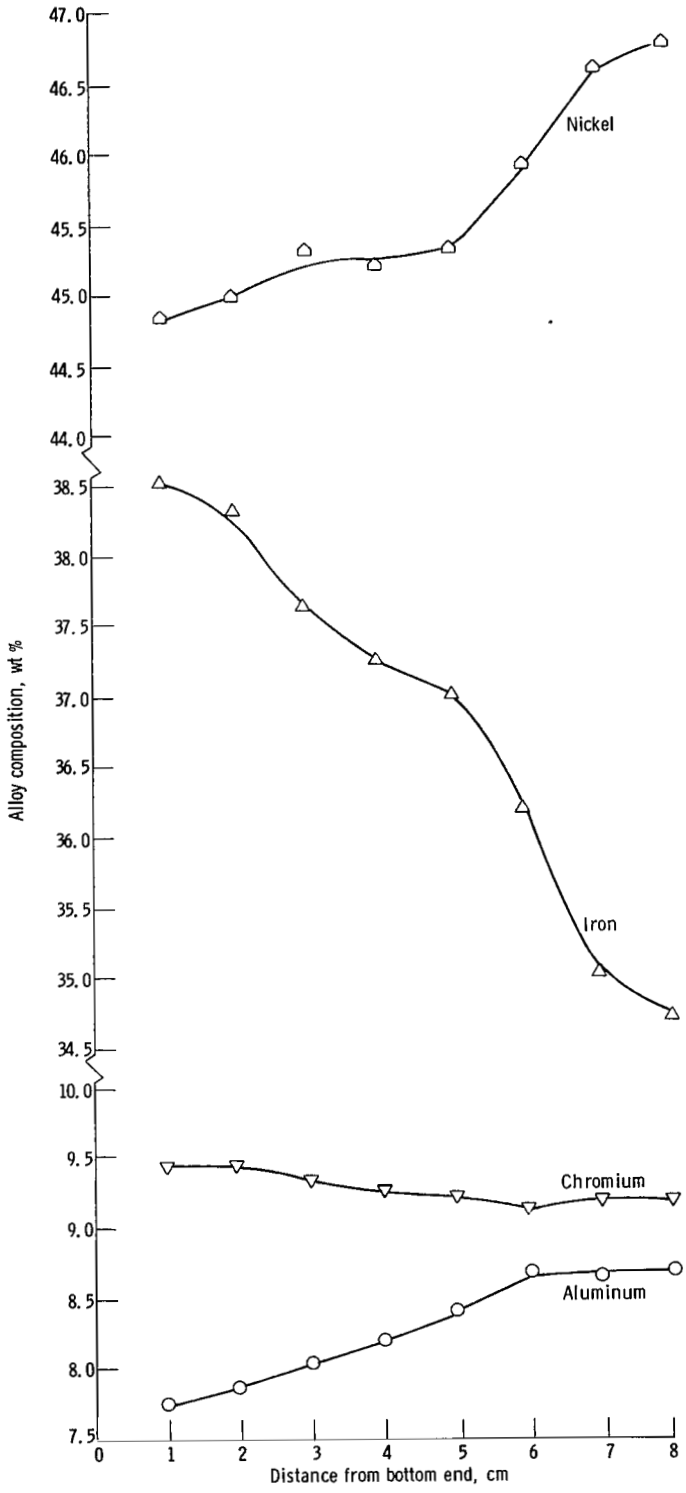

Figure 4. - Change in alloy (Ni-36Fe-9.3Cr-8.7Al) composition along the directionally solidified bar length.

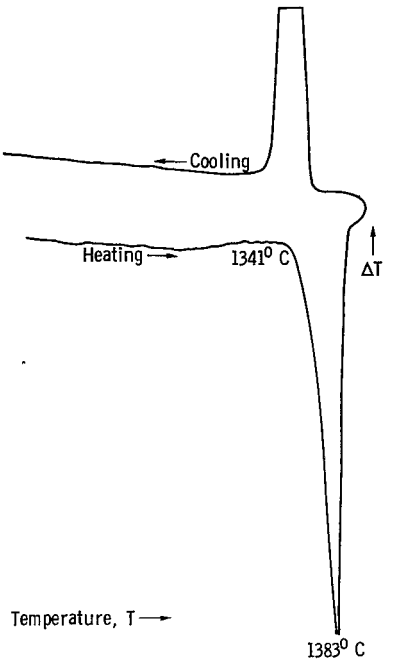

Figure 5. - Differential thermal analysis of (DTA) trace of γ-β eutectic alloy (Ni-37. 4Fe-10. 0Cr-9. 6Al).

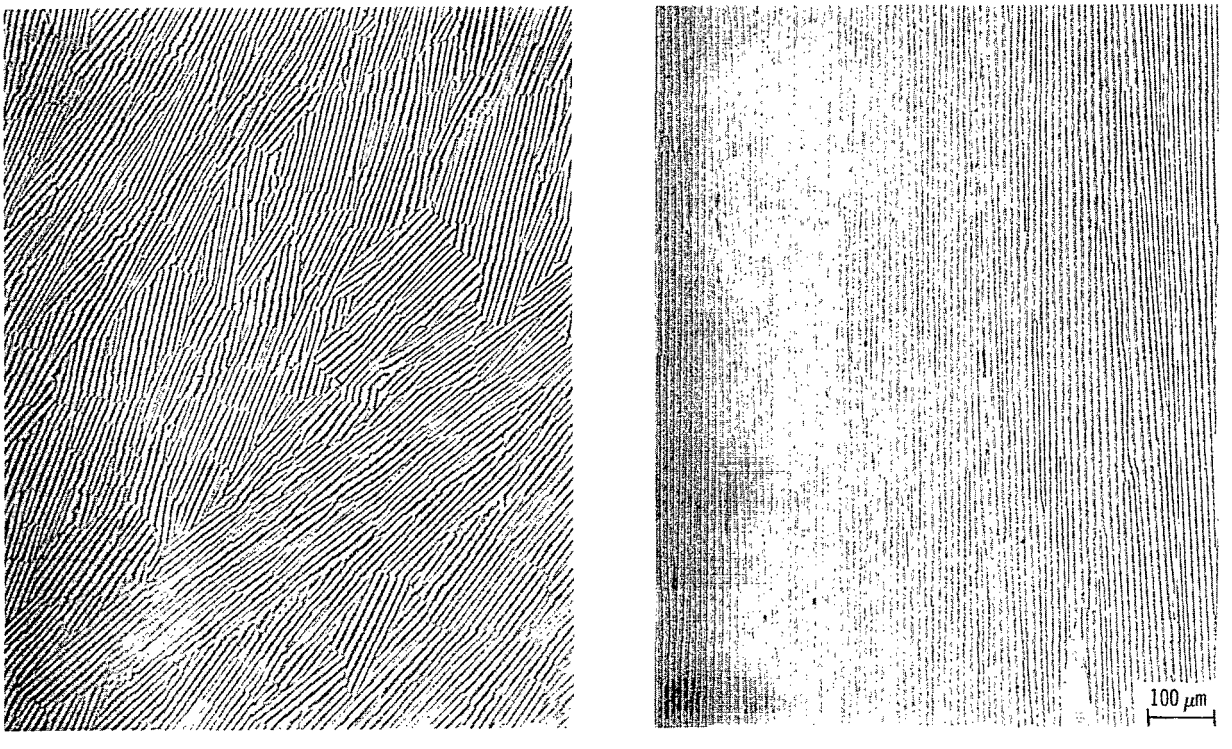

(a) Transverse.

(b) Longitudinal.

Figure 6. - Microstructure of DS γ-β eutectic alloy (Ni-37.4Fe-10.0Cr-9.6Al). (Light areas in microphotographs show γ material; dark, β.)

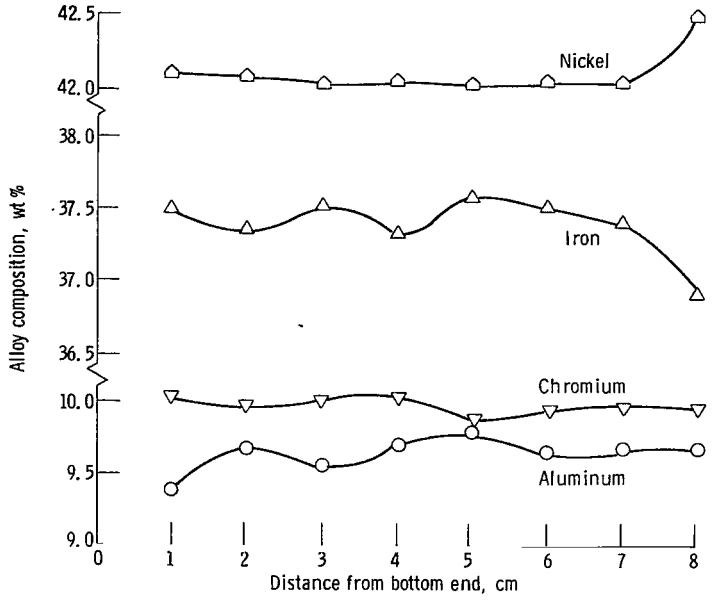

Figure 7. - Change in alloy (Ni-37.4Fe-10.0Cr-9.6Al) composition along the directionally solidified γ-β bar length.

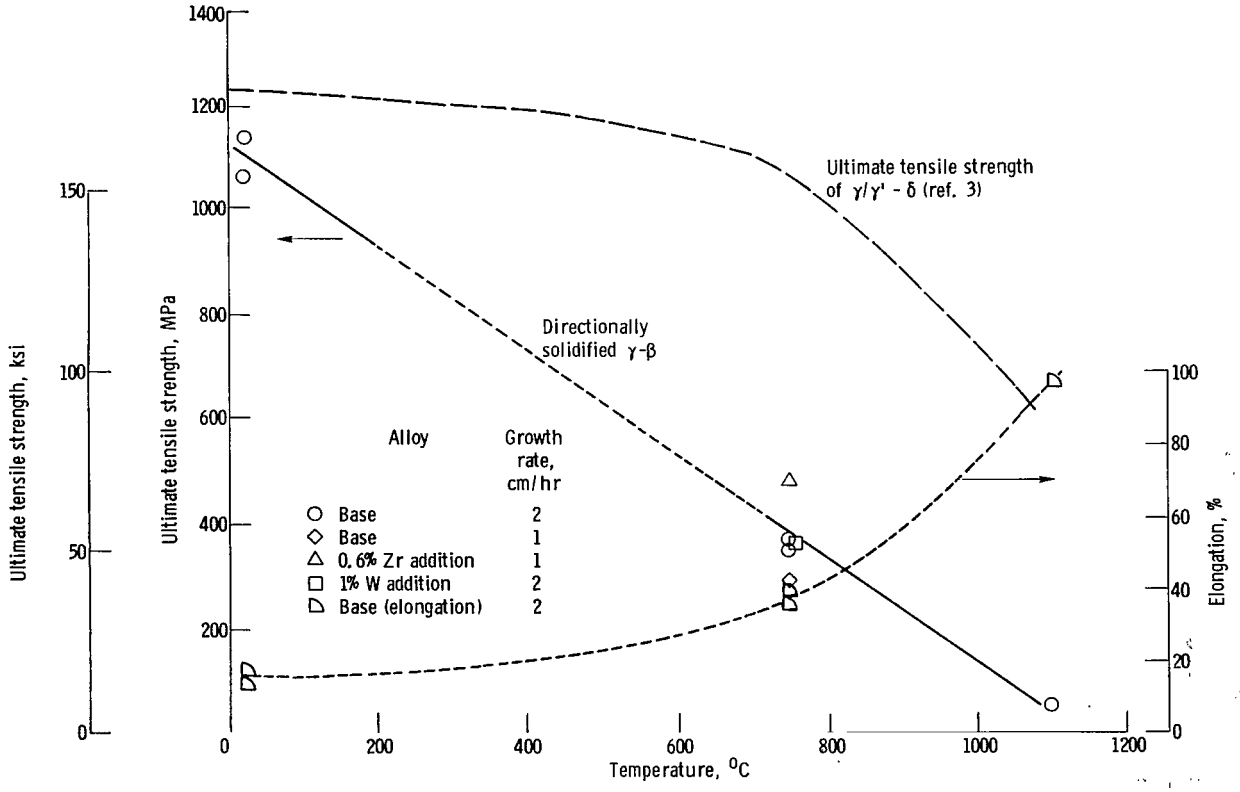

Figure 8. - Temperature dependence of tensile properties of directionally solidified γ-β eutectic alloy.

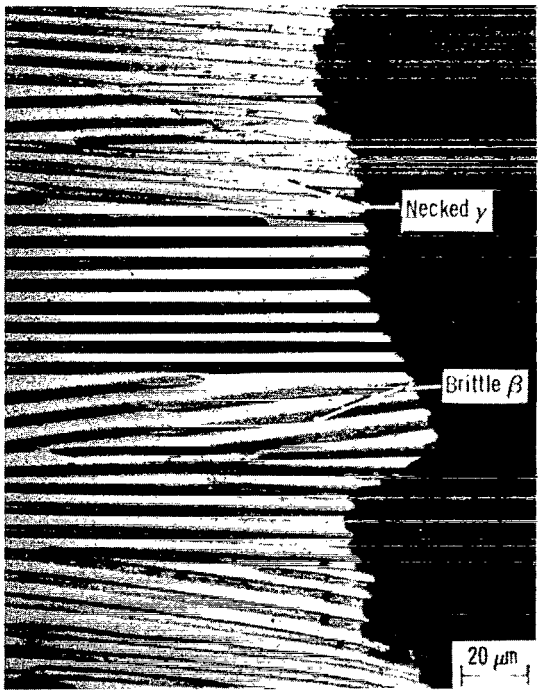

(a) Room temperature (Light micrograph, longitudinal section).

(b) Room temperature (SEM micrograph-transverse section).

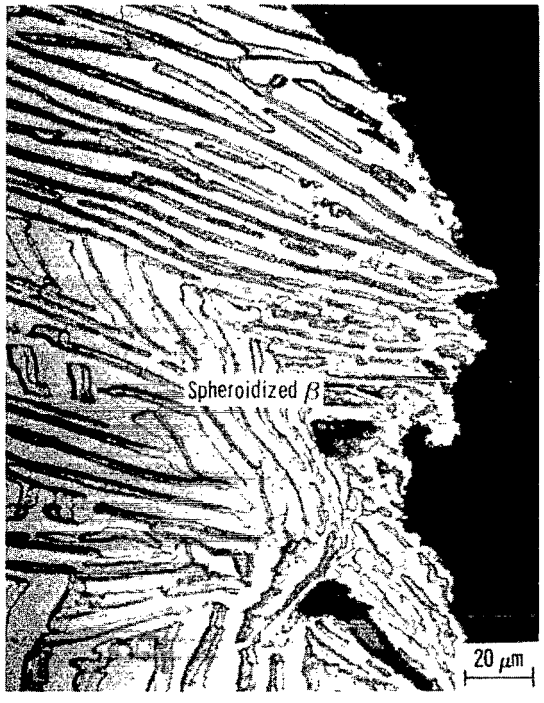

(c) Temperature, 1100° C (Light micrograph, longitudinal section).

Figure 9. - Effect of temperature on tensile fracture morphology of directionally solidified γ-β alloy.

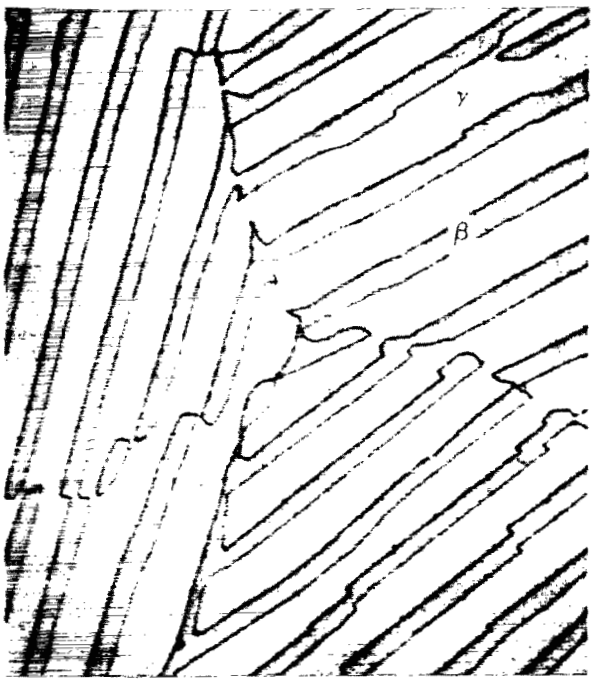

(a) Directionally solidified γ-β.

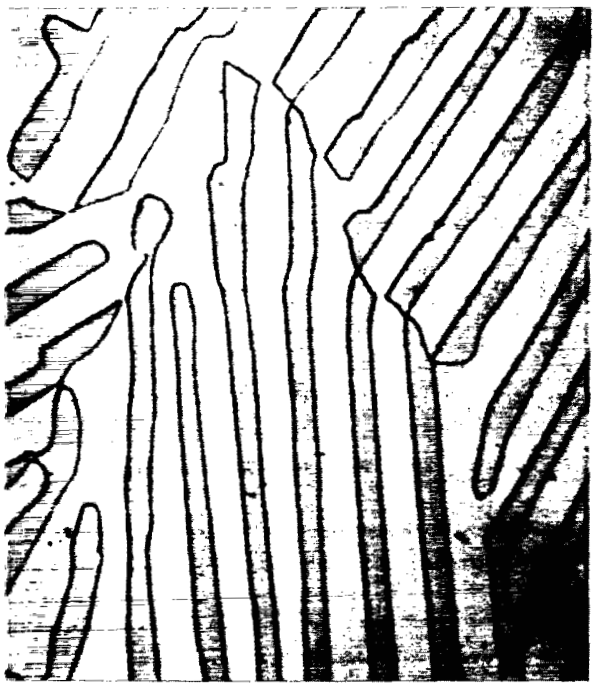

(b) Thermally cycled γ-β.

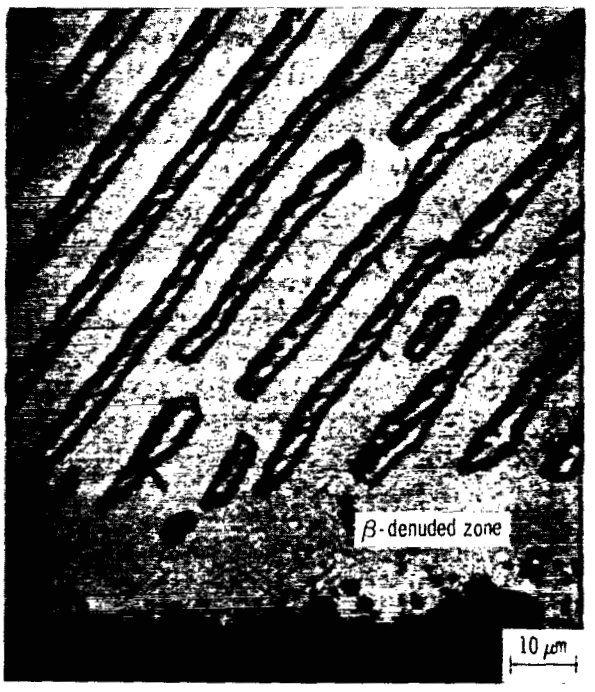

(c) β-denuded zone at surface.

Figure 10. - Effect of thermal cycling on microstructure of directionally solidified γ-β eutectic alloy. Transverse sections; 1800 3-minute cycles between 1100° and 425° C.

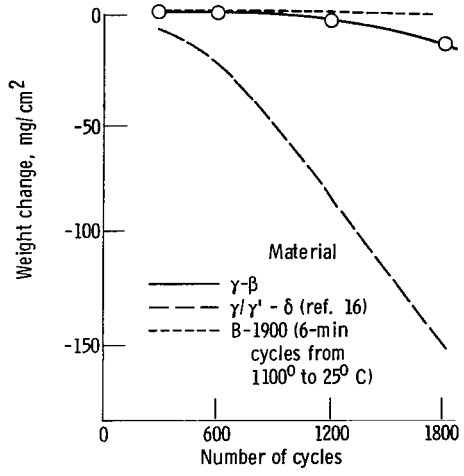

Figure 11. - Specific weight change of directionally solidified γ-β eutectic alloy due to thermal cycling in Mach 0.3 oxidation-erosion burner rig.

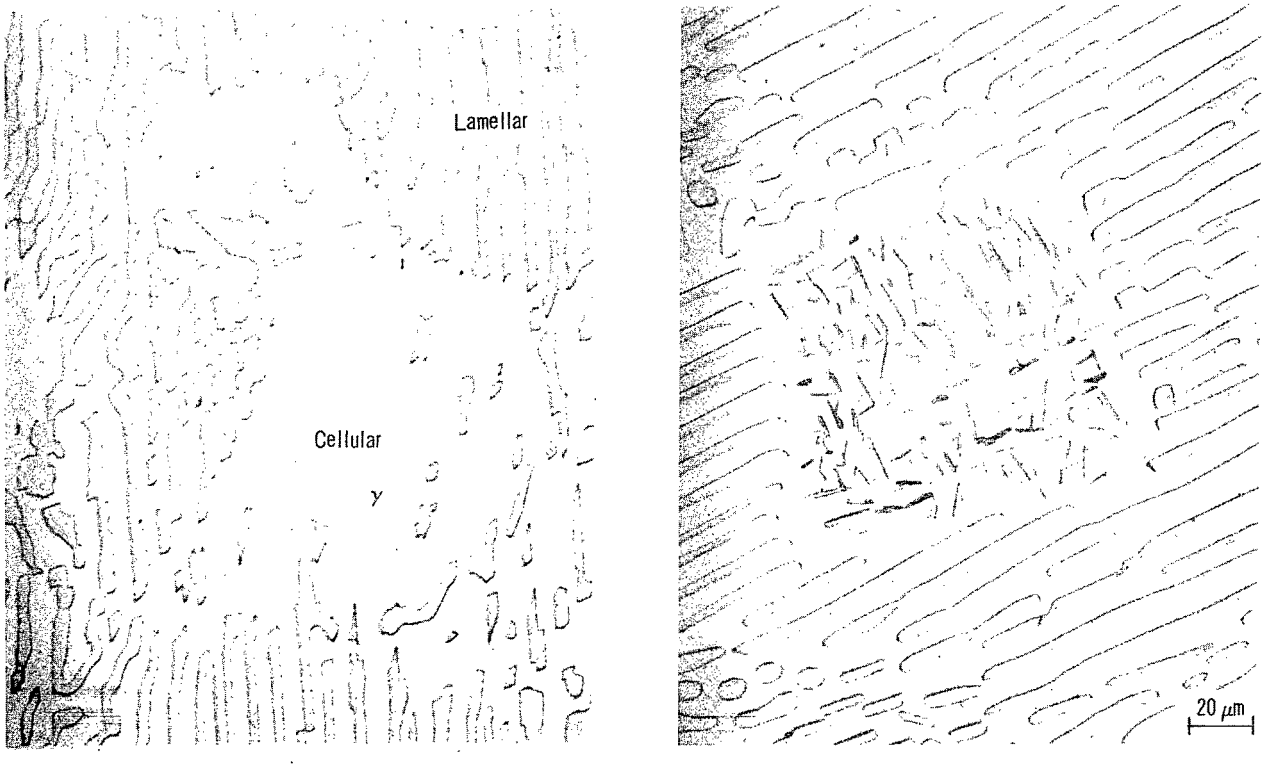

(a) Directionally solidified.

(b) Directionally solidified and thermally cycled.

Figure 12. - Effect of thermal cycling on the cellular microstructure of directionally solidified γ-β eutectic alloy. 1800, 2.5-minute cycles between 1100° and 425° C.

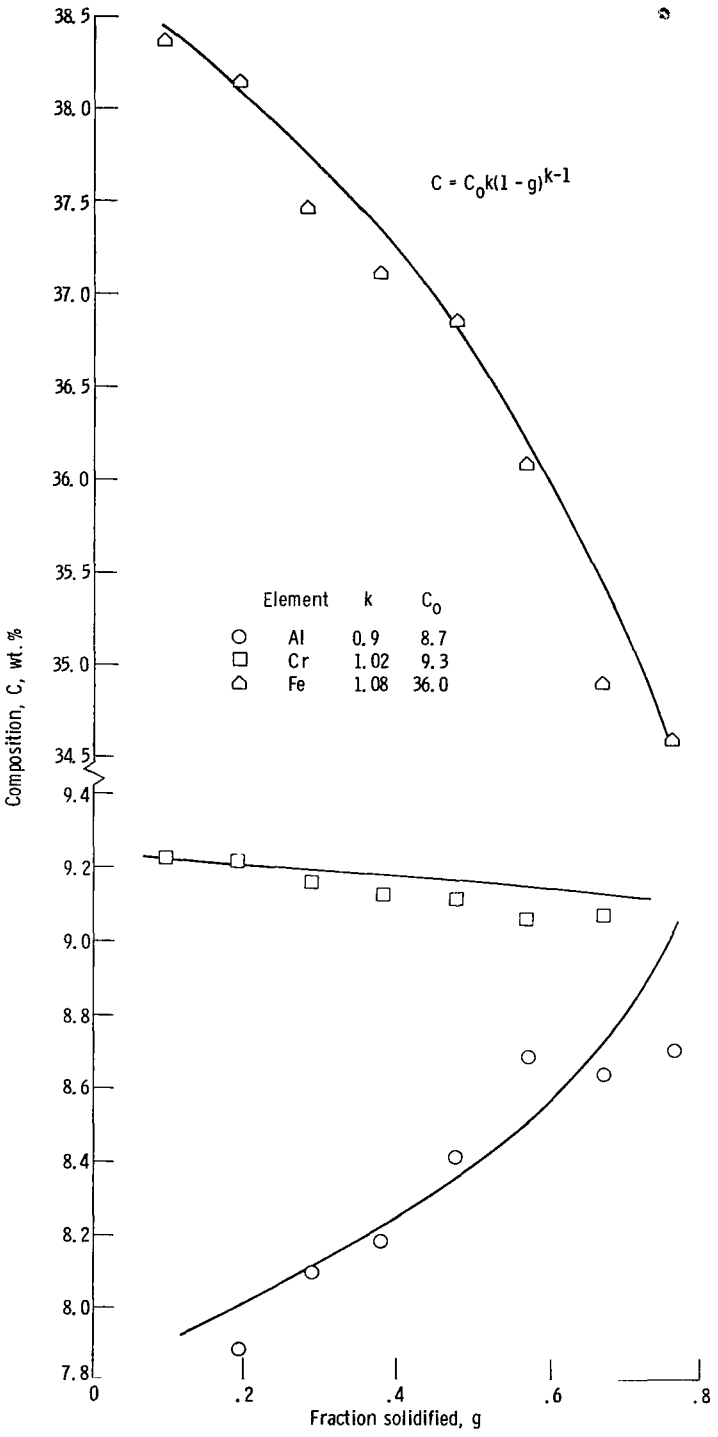

Figure 13. - Composition profiles for aluminum, chromium, and iron as compared with theoretical curves for normal freezing for Ni-36.0Fe-9.3Cr-8.7Al(wt. %).

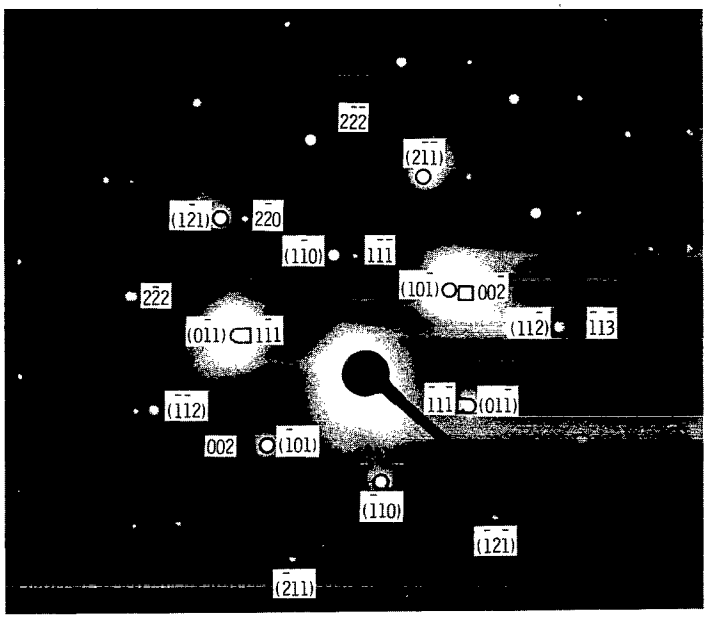

Figure 14. - Electron diffraction pattern at γ - β interface. Transverse section; $[110]_\gamma \parallel [111]_\beta \parallel$ growth direction, $(1\bar{1}1)_\gamma \parallel (0\bar{1}1)_\beta$.

"The aeronautical and space activities of the United States shall be conducted so as to contribute . . . to the expansion of human knowledge of phenomena in the atmosphere and space. The Administration shall provide for the widest practicable and appropriate dissemination of information concerning its activities and the results thereof."

—NATIONAL AERONAUTICS AND SPACE ACT OF 1958

NASA SCIENTIFIC AND TECHNICAL PUBLICATIONS

TECHNICAL REPORTS: Scientific and technical information considered important, complete, and a lasting contribution to existing knowledge.

TECHNICAL NOTES: Information less broad in scope but nevertheless of importance as a contribution to existing knowledge.

TECHNICAL MEMORANDUMS: Information receiving limited distribution because of preliminary data, security classification, or other reasons. Also includes conference proceedings with either limited or unlimited distribution.

CONTRACTOR REPORTS: Scientific and technical information generated under a NASA contract or grant and considered an important contribution to existing knowledge.

TECHNICAL TRANSLATIONS: Information published in a foreign language considered to merit NASA distribution in English.

SPECIAL PUBLICATIONS: Information derived from or of value to NASA activities. Publications include final reports of major projects, monographs, data compilations, handbooks, sourcebooks, and special bibliographies.

TECHNOLOGY UTILIZATION PUBLICATIONS: Information on technology used by NASA that may be of particular interest in commercial and other non-aerospace applications. Publications include Tech Briefs, Technology Utilization Reports and Technology Surveys.

Details on the availability of these publications may be obtained from:

SCIENTIFIC AND TECHNICAL INFORMATION OFFICE

NATIONAL AERONAUTICS AND SPACE ADMINISTRATION

Washington, D.C. 20546